

# Loss tolerant cross-Kerr enhancement via modulated squeezing

Ankit Tiwari,<sup>1</sup> Daniel Burgarth,<sup>2</sup> Linran Fan,<sup>3</sup> Saikat Guha,<sup>4</sup> and Christian Arenz<sup>1</sup>

<sup>1</sup>*School of Electrical, Computer, and Energy Engineering,  
Arizona State University, Tempe, Arizona 85287, USA*

<sup>2</sup>*Department Physik, Friedrich-Alexander-Universität Erlangen-Nürnberg, Staudtstraße 7, 91058 Erlangen, Germany*

<sup>3</sup>*Chandra Department of Electrical and Computer Engineering,  
The University of Texas at Austin, Austin, TX, USA*

<sup>4</sup>*Department of Electrical and Computer Engineering, University of Maryland,  
8228 Paint Branch Dr, College Park, MD 20742, USA*

We develop squeezing protocols to enhance cross-Kerr interactions. We show that through alternating between squeezing along different quadratures of a single photonic mode, the cross-Kerr interaction strength can be generically amplified. As an application of the squeezing protocols we discuss speeding up the deterministic implementation of controlled phase gates in photonic quantum computing architectures. We develop bounds that characterize how fast and strong single-mode squeezing has to be applied to achieve a desired gate error and show that the protocols can overcome photon losses. Finally, we discuss experimental realizations of the squeezing strategies in optical fibers and nanophotonic waveguides.

*Introduction* — Photonic systems are among the most promising platforms for realizing a fault-tolerant quantum computer [1]. Qubits encoded in the presence of a single photon in one of two orthogonal modes, along with linear optical elements, such as phase shifters and beam splitters, and some non-linear process, enable universal quantum computing [2, 3]. The non-linear process required to implement controlled phase gates on such *dual rail* photonic qubits is the cross-Kerr interaction [4].

Unfortunately, the in-line Kerr effect for optical frequencies in non-linear material platforms used in photonic systems is typically extremely weak. Consequently, imparting a full  $\pi$  phase shift for single-photon level signals [5] needed to realize a controlled phase gate is deterministically not achievable, which poses one of the main challenges for realizing a photonic quantum computer. The way the photonic quantum computing community has mitigated this shortcoming is by eliminating the in-line Kerr phase by the injection of ancilla single photons into an otherwise linear optical circuit [6], leveraging an effect termed Boosted Bell State Measurement [7]. Variants of this architecture underlie the platform of PsiQuantum, a company that is pursuing fault-tolerant photonic quantum computing [8]. The shortcoming of this workaround is that despite the *boosting* of the success probability of two-qubit gates such as the controlled phase gate, the architecture still relies on probabilistic gates, hence massive amounts of multiplexed heralded operations, which drive the resource overheads to be astronomically high.

In this work, we address the problem of weak cross-Kerr interactions by developing protocols that amplify the cross-Kerr interaction through squeezing. This is achieved by interspersing the free evolution by single-mode squeezing transformations along different quadratures (i.e., the squeezing direction is modulated as a function of time). We show that in this way the cross-Kerr interaction strength between multiple optical modes of a quantum system can be generically enhanced.

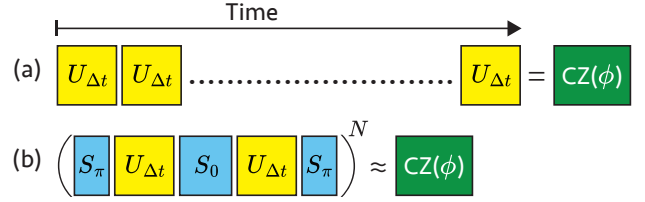


Figure 1. Schematic representation of the squeezing protocols that are developed in this work to speed. A controlled phase gate  $\text{CZ}(\phi)$  (green) can be (deterministically) implemented by (a) repeating the evolution  $U_{\Delta t}$  generated by the cross-Kerr interaction over a time interval  $\Delta t$  (yellow). Since the cross-Kerr interaction is typically weak, this process is unpractical as the time scale required to impart a full  $\pi$  phase shift is beyond the coherence time of the system. Instead, in (b) the cross-Kerr evolution  $U_{\Delta t}$  is interspersed with single-mode squeezing transformations  $S_{\theta}$  (blue) along different quadratures ( $\theta = 0, \pi$ ) to enhance the cross-Kerr interaction. In this way only a few repetitions of  $U_{\Delta t}$  are required to implement  $\text{CZ}(\pi)$ . The resulting (Trotter) error is determined by the spacings  $\Delta t = \frac{t}{2^N}$  of  $S_{\theta}$ .

As depicted in Fig. 1, as an application of the modulated squeezing strategies, we consider speeding up the implementation of controlled phase gates in photonic quantum computing. We develop an error bound for the gate error that characterizes how fast squeezing has to be applied to achieve a desired speed-up. We go on to show that the developed squeezing sequences can outperform photon losses when sufficiently fast and strong squeezing is available. Finally, we discuss experimental implementations of the protocols in optical fibers and nanophotonic waveguides. We argue that a significant improvement of currently observed controlled phase shifts is possible through the developed sequences with current technology.

*Enhancing cross-Kerr interactions through Hamiltonian amplification* — The cross-Kerr interaction between

two photonic modes described by quantum harmonic oscillators is described by the Hamiltonian

$$H = \chi a^\dagger a b^\dagger b, \quad (1)$$

where we set  $\hbar = 1$ ,  $\chi$  is the cross-Kerr interaction strength and  $a, a^\dagger$  and  $b, b^\dagger$  are the bosonic annihilation and creation operators of each mode.

Several strategies exist that use squeezing to enhance interactions involving quantum harmonic oscillators [9]. However, these strategies typically require fine tuning to the system's parameters and often rest on assumptions about the initial state of the system and the parameter regimes considered. For example, the strategy developed in [10] to enhance cross-Kerr interactions uses single-mode squeezing and phase shifters that are precisely tuned to the cross-Kerr strength  $\chi$  and requires a certain class of initial states. These requirements make it challenging to implement the protocol in the laboratory without introducing more noise and photon losses. A recently introduced approach called *Hamiltonian amplification* [11, 12] can overcome these challenges. This strategy amplifies interactions by interspersing the free evolution with squeezing transformations along orthogonal quadratures to obtain an interaction enhancement independent of the initial state and parameter details.

Consider modifying the dynamics  $U_{\Delta t} = e^{-iH\Delta t}$  generated by the cross-Kerr interaction (1) by alternating in time intervals  $\Delta t = \frac{t}{2N}$  between squeezing a single mode along different quadratures described by the squeezing transformation  $S_\theta = \exp[\frac{r}{2}(a^2 e^{i\theta} - a^{\dagger 2} e^{-i\theta})]$ . Here,  $\theta$  is the squeezing angle that describes along which quadrature the mode is squeezed. We omit the explicit dependence of  $S_\theta$  on the squeezing parameter  $r$  that describes the squeezing strength. If the alternation is done sufficiently fast, described by the (Trotter) limit,

$$\lim_{N \rightarrow \infty} \left( S_0^\dagger U_{\Delta t} S_0 S_\pi^\dagger U_{\Delta t} S_\pi \right)^N = e^{-i \cosh(2r) H t}, \quad (2)$$

the cross-Kerr interaction is amplified by a factor  $\lambda = \cosh(2r)$  that increases exponentially in the squeezing strength  $r$ . We note that amplifying  $H$  by  $\lambda$  through the sequence (2) does not require knowledge of the cross-Kerr strength  $\chi$  and is independent of the initial state of the system. By simultaneously squeezing both modes, larger amplification factors  $\lambda^2$  can be achieved, which we discuss next.

Since in the limit of infinitely fast alternation ( $N \rightarrow \infty$ ) the resulting dynamics is governed by a map of the form  $M(H) = \frac{1}{2}(S_0^\dagger H S_0 + S_\pi^\dagger H S_\pi) = \lambda H$ , composing two maps  $M_a$  and  $M_b$  that describe squeezing each mode  $a$  and  $b$ , respectively,  $M_a(M_b(H)) = \lambda^2 H$ , achieves amplification of the cross-Kerr interaction by a factor  $\cosh^2(2r)$ . The explicit form of the resulting squeezing sequence is given in the supplemental material [13]. In general, composing maps of the form  $M$  allows for amplifying generic multi-mode cross-Kerr interactions [14, 15]. Consider the

cross-Kerr interaction

$$H = \chi_n \prod_{j=1}^n a_j^\dagger a_j, \quad (3)$$

between  $n$  modes described by the bosonic annihilation and creation operators  $a_j$  and  $a_j^\dagger$ . If we denote by  $M_j$  the map that describes amplifying the term  $a_j^\dagger a_j$  by a factor  $\cosh(2r)$  through applying squeezing to the  $j$ th mode, then the composition,

$$\prod_{j=1}^n M_j(H) = \cosh^n(2r) H \quad (4)$$

allows for amplifying the multi-mode cross-Kerr interaction (3) by a factor  $\cosh^n(2r) \approx \cosh(2nr)$  (for  $r \gg 1$ ). Thus, the amplified multi-mode cross-Kerr strength increases exponentially in the number of modes  $n$  involved, while the single-mode squeezing strength  $r$  can remain fixed.

In order to investigate how fast squeezing along different quadratures needs to be applied to achieve the desired enhancement, we consider speeding up the implementation of a controlled phase gate in photonic quantum computing.

*Speeding up the implementation of controlled phase gates in photonic quantum computing* — The cross-Kerr interaction can be used to implement a controlled phase gate  $\text{CZ}(\phi) = \text{diag}(1, 1, 1, e^{-i\phi})$  over dual rail qubits [16, 17]. Indeed, the cross-Kerr evolution  $U_t$  creates a controlled phase gate in the computational subspace  $\mathcal{C} = \{|00\rangle, |10\rangle, |01\rangle, |11\rangle\}$ , where  $|n\rangle$ ,  $n = 0, 1$ , denote the eigenstates of  $a^\dagger a$  and  $b^\dagger b$ . The controlled phase shift  $\phi = \chi t$  is determined by the cross-Kerr interaction strength  $\chi$  and the evolution time  $t$ . As such, in order to impart a desired phase shift, a sufficiently long coherent evolution is needed, depending on the cross-Kerr strength  $\chi$ . Thus, if  $\chi$  is amplified through the sequence in (2), a desired phase shift can be obtained for shorter evolution times. The error that is introduced due to the Trotterization in (2) is determined by the time interval  $\Delta t$  of the Trotterization.

Using recently developed state-dependent Trotter bounds for infinite dimensional systems [18–20], in [13] we show that the gate error,

$$\epsilon_N(\phi) = \left\| \text{CZ}(\phi) - P \left( S_0^\dagger U_{\Delta t} S_0 S_\pi^\dagger U_{\Delta t} S_\pi \right)^N P \right\|_{\text{HS}}, \quad (5)$$

for implementing a controlled phase shift  $\phi$  where  $P$  is the projector into the computational subspace  $\mathcal{C}$  and  $\|\cdot\|_{\text{HS}}$  denotes the Hilbert-Schmidt norm is upper bounded by

$$\epsilon_N(\phi) \leq \frac{\chi^2 t^2 \cosh^2(2r)}{8N} f(r). \quad (6)$$

For  $r \gg 1$ , the function  $f(r)$  is approximately constant, such that  $\epsilon = \mathcal{O}\left(\frac{\phi^2}{N}\right)$  where  $\phi = \chi t \cosh(2r)$  is the

amplified phase shift. Consequently, for large squeezing strengths the Trotter error is approximately upper bounded by a factor that is independent of the amplification factor  $\lambda$ . As such, the Trotter error can be controlled by increasing the number of Trotter steps  $N$ , *independently* of how much the cross-Kerr interaction strength  $\chi$  needs to be amplified to obtain the desired phase shift  $\phi$ . The tightness of the bound (6) is analyzed in more detail in [13].

*Overcoming photon losses* — We now turn to the question of how the amplification of the cross-Kerr interaction is influenced by photon losses. Typically, photon losses are described by a quantum channel  $\exp(\eta t(\mathcal{D}_a + \mathcal{D}_b))$  where  $\mathcal{D}_L(\cdot) = L(\cdot)L^\dagger + \frac{1}{2}(L^\dagger L(\cdot) + (\cdot)L^\dagger L)$  is a Lindblad operator that describes photon losses for each mode  $a$  and  $b$ , and  $\eta t$  is the overall loss rate. To gain some intuition for how amplification through the squeezing sequences (2) can overcome photon losses, we start by assuming that photon losses occur between the squeezing transformations  $S_\theta$  and the Trotterized cross-Kerr evolution  $U_{\Delta t}$ . In this case, photon losses can accumulate less compared to the case where squeezing is not present. This is because the amplification sequences can be shorter than the sequence that is formed by repeating the cross-Kerr evolution to obtain a desired phase shift, as schematically represented in Fig. 1. Consequently, in the amplified case the loss channel is less frequently applied, which results in less overall photon loss.

However, typically squeezing introduces more losses and also results in heating [21]. In order to capture these effects, we proceed by considering a loss model in which photon losses also occur during the cross-Kerr evolution. With further details found in [13], this is achieved by weakly coupling each mode via a beam-splitter interaction to auxiliary modes that are assumed to be in the vacuum state [22]. After each time interval  $\Delta t$  the auxiliary modes are traced out to obtain a quantum channel  $\mathcal{E}_{\Delta t}^{(j)}$  whose explicit form is given in [13]. Here,  $j$  labels the squeezing transformation that is applied before and after  $\Delta t$ . We show that when squeezing is applied to both modes, for sufficiently many Trotter steps  $N$  the resulting sequence  $(\prod_j \mathcal{E}_{\Delta t}^{(j)})^N$  is given by the quantum channel

$$\mathcal{E}_t = \exp([\cosh^2(2r)\mathcal{H} + \cosh^2(r)\mathcal{L}_l + \sin^2(r)\mathcal{L}_h]t) \quad (7)$$

where  $\mathcal{H} = -i[H, \cdot]$  is the super operator describing the cross-Kerr interaction,  $\mathcal{L}_l = \eta(\mathcal{D}_a + \mathcal{D}_b)$  describes the amplified photon losses and  $\mathcal{L}_h = \eta(\mathcal{D}_{a^\dagger} + \mathcal{D}_{b^\dagger})$  are heating processes. We note that for  $r = 0$ , i.e., when no squeezing is present, the resulting quantum channel  $\mathcal{E}_t = \exp(\mathcal{H} + \mathcal{L}_l)$  describes photon losses that occur during the cross-Kerr evolution. We further remark that directly modeling photon losses during the cross-Kerr evolution through  $\mathcal{L}_l$  yields for sufficiently large  $N$  the same quantum channel given in (7).

When squeezing is applied to both modes, the cross-Kerr interaction is amplified by  $\cosh^2(2r)$  while losses and heating process occur with rates  $\propto \cosh^2(r)$  and  $\propto$

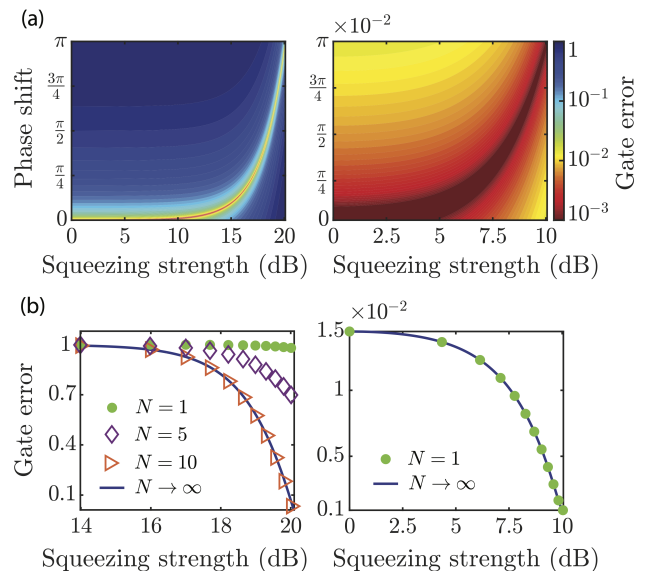


Figure 2. Gate error for implementing a controlled phase gate in the presence of photon losses when the cross-Kerr interaction is amplified through single-mode squeezing applied to both modes. The bare phase shift  $\chi t = 1.2 \times 10^{-3}$  and loss rate  $\eta t = 5.76 \times 10^{-4}$  dB was chosen according to the parameters reported in optical fibers [23, 24]. The color maps in (a) show the gate error as a function of the squeezing strength  $r$  for phase shifts up to  $\phi = \pi$  (left panel) and  $\phi = \frac{\pi}{100}$  (right panel) based on the quantum channel in Eq. (7) that is obtained in the limit  $N \rightarrow \infty$ . In (b) the gate error is plotted for a fixed phase shift  $\phi = \pi$  (left) and  $\phi = \frac{\pi}{100}$  (right) for different Trotter steps  $N = 1$  (green circles),  $N = 5$  (purple diamonds) and  $N = 10$  (orange triangles). In all cases, the gate error was normalized to 1 by dividing by its largest value.

$\sinh^2(r)$ , respectively. We observe that the cross-Kerr interaction is more enhanced than the loss and heating processes, which can be traced back to the linear coupling of each mode via the beam splitter interaction to the auxiliary modes. As such, a full  $\pi$  phase shift is obtained at a shorter time  $t = \frac{\pi}{\chi \cosh^2(2r)}$  at which photon losses and heating processes occur with smaller rates  $\approx e^{-2r} \frac{\eta}{\chi}$ .

Loss and heating processes can be even more outperformed when  $n$ -mode cross-Kerr interactions (3) are used to implement controlled phase gates. Assuming again that each mode couples linearly via a beam splitter interaction to auxiliary vacuum modes, the time to implement a full  $\pi$  phase shift is then further reduced to  $t = \frac{\pi}{\chi \cosh^n(2r)}$  while at  $t$  loss and heating processes occur with rates  $\approx e^{-2nr} \frac{\eta}{\chi}$ .

In Fig. 2 we investigate the loss model given by the quantum channel  $\mathcal{E}_t$  in Eq. (7). For the numerical simulations we chose  $\chi t = 1.2 \times 10^{-3}$  and  $\eta t = 5.76 \times 10^{-4}$  dB, which correspond to the phase shift and loss rates reported for optical (photonic crystal) fibers in [23] and [24], respectively. Throughout this work, we express phase shifts in radians.

In Fig. 2 (a) we plot the gate error  $\|\mathcal{CZ}_\phi - \mathcal{P}\mathcal{E}_t\mathcal{P}\|_{\text{HS}}$

as a function of the squeezing strength  $r$  for different phase shifts, i.e., up to a full  $\pi$  phase shift (left panel) and up to a  $\frac{\pi}{100}$  phase shift (right panel). Here,  $\mathcal{CZ}_\phi(\cdot) = \text{CZ}(\phi)(\cdot)\text{CZ}^\dagger(\phi)$  and  $\mathcal{P} = P(\cdot)P$  are the quantum channel and the super operator that describe the controlled phase gate and the projection into the computational subspace, respectively. In the numerical simulations, we used the matrix representation of the quantum channels and superoperators obtained from row vectorization [25] of the density operator.

The color map plots in Fig. 2 (a) suggest that without amplification only phase shifts  $\phi \leq \frac{\pi}{100}$  can be achieved with gate errors  $\epsilon \leq 10^{-2}$ . The situation changes when the cross-Kerr interaction is amplified by applying squeezing to both modes. A full  $\pi$  phase shift with  $\epsilon \approx 10^{-2}$  can be obtained when enough single-mode squeezing  $r \approx 20$  dB is available. We expect that the amount of single-mode squeezing needed to impart a full  $\pi$  phase shift can be further reduced to  $r \approx 14$  dB when cross-Kerr interactions across three modes are used to implement controlled phase gates. The colormap plot shown in the right panel in Fig. 2 (a) shows the phase shift improvements that are possible in existing platforms. We observe that with a squeezing strength of  $r \approx 8$  dB, achievable in optical fibers [26] and nanophotonic waveguides [27], about an order of magnitude improvement in the gate error to create a  $\frac{\pi}{100}$  phase shift is possible.

In Fig. 2 (b) we study the effect of Trotterization for a fixed phase shift  $\phi = \pi$  (left panel) and  $\phi = \frac{\pi}{100}$  (right panel). Fig 2 (b) shows the gate error  $\|\mathcal{CZ}_\phi - \mathcal{P}(\prod_j \mathcal{E}_{\Delta t}^{(j)})^N \mathcal{P}\|_{\text{HS}}$  for  $N = 1$  (green circles),  $N = 5$  (purple diamonds) and  $N = 10$  (orange triangles) Trotter steps. For comparison, we show the gate error determined for  $N \rightarrow \infty$  by the quantum channel  $\mathcal{E}_t$  in Eq. (7) as a blue line. We see that already for  $N = 1$  Trotter steps the behavior of the gate error is remarkably well described by the channel  $\mathcal{E}_t$  when small phase shifts are considered (right panel). However, from the left panel in Fig. 2 we see that to obtain a full  $\pi$  phase shift, more Trotter steps  $N$  are needed to achieve the gate errors determined by  $\mathcal{E}_t$ . For more details regarding the behavior of the evolution as a function of  $N$  we refer to [13].

*Potential experimental implementations* — Experimental platforms in which cross-Kerr modulated phase shifts can be observed while photon losses remain low and sufficiently strong single-mode squeezing is available are ideal candidates for implementing the developed squeezing sequences. These requirements are for example met in optical fibers [23, 26, 28–34] and nanophotonic waveguides [27, 35–42] where the spacing of the squeezers (i.e., in the fiber or waveguide) determines the time interval  $\Delta t$  of the Trotterization.

In particular, the parameters used in the numerical simulations shown in Fig. 2 were taken from an experimental setting that utilizes a rubidium vapour-filled

hollow-core photonic bandgap fiber [23]. In this platform, a cross-Kerr modulated phase shift of  $3 \times 10^{-4}$  is produced over a  $\approx 9$  cm long fiber. Assuming that this phase shift can be replicated four times within a single Trotter step in the low-loss optical fiber described in [24], we estimated the total loss rate used in the numerical simulations as  $\eta t = 5.76 \times 10^{-4}$  dB per mode [43]. In a recent work [26] a squeezing strength of  $r = 7.5$  dB has been generated in optical fiber type systems, which would within the considered parameter regime allow for improving the phase shifts currently achievable in these systems by about an order of magnitude with a gate error of  $\epsilon \leq 10^{-2}$  (see Fig. 2 (b)). As such, we expect that significantly larger controlled phase shifts may be achievable in optical fibers through the developed squeezing protocols.

Nanophotonic waveguides are also a viable platform for implementing the cross-Kerr amplification sequences. Both, squeezed light [35–37] and cross-Kerr modulated phase shifts [38–40] can be generated in these systems. Squeezed light with a squeezing strength as large as  $r = 8$  dB has been generated in nanophotonic waveguides [27], which corresponds to an amplification factor of  $\cosh^2(2r) \approx 10.45$ . Meanwhile, cross-Kerr modulated phase shifts of the order of  $10^{-7}$  are expected in nanophotonic waveguides with waveguide losses  $\approx 2$  dB/cm [44]. In recent studies a significant reduction in photon losses has been demonstrated in lithium niobate and silicon nitride waveguides, achieving loss rates of  $4 \times 10^{-2}$  dB/cm [45] and  $3.4 \times 10^{-4}$  dB/cm [42], respectively. We expect that further improvements in hybrid systems [41, 46] will pave the way for achieving large controlled phase shifts in nanophotonic waveguides through the protocols developed here.

*Conclusions* — We have developed single-mode squeezing protocols that allow for enhancing cross-Kerr interactions. In particular, we showed that the multi-mode cross-Kerr interaction strength can be amplified by alternating between squeezing along orthogonal quadratures of a single mode. We found that the interaction enhancement scales exponentially in the number of modes involved. This observation may allow for overcoming challenges in systems where only small single-mode squeezing is available, but squeezing can simultaneously be applied to all modes that are coupled via multi-mode cross-Kerr interactions.

As a key application of the developed squeezing protocols, we considered the deterministic implementation of controlled phase gates in photonic quantum computing. We showed that the hard-to-realize strong cross-Kerr interaction at single-photon levels needed for realizing a controlled phase gate could be realized in a photon loss-tolerant. We also discussed concrete realizations of the proposed concept in optical fibers and nanophotonic waveguides, which suggests that the implementation of the scheme is feasible with current technology.

In future work, it would be instructive to perform a thorough resource evaluation to realize fault-tolerant

quantum computing over dual-rail photonic qubits using the developed protocols, assuming realistic devices, and compare that with the conventional approach that rests on multiplexed probabilistic resource-state preparation and fusion-based quantum computations [8]. Furthermore, the principles in this work could be leveraged to amplify other non-Gaussian Hamiltonians such as the cubic-phase Hamiltonian, which has applications in GKP-qubit photonic quantum computing [47], more efficiently compared with the alternative method of probabilistic heralded-multiplexed preparation of cubic-phase ancillas [48]. Our work could also find applications broadly in the universal bosonic circuit synthesis prob-

lem, which could help realize quantum optimal measurements for applications such as optical codeword discrimination for attaining the Holevo limit of optical communications capacity [49, 50], and designing non-Gaussian receivers for distributed photonic sensors [51, 52].

*Acknowledgements* — AT and SG thank Chaohan Cui for helpful discussions. SG, CA and AT acknowledge funding support from the Air Force Office of Scientific Research (AFOSR) under the award FA9550-24-1-0139. CA and AT acknowledge support from the Quantum Collaborative and the SenSip Center at Arizona State University.

- 
- [1] P. Kok, W. J. Munro, K. Nemoto, T. C. Ralph, J. P. Dowling, and G. J. Milburn, Linear optical quantum computing with photonic qubits, *Rev. Mod. Phys.* **79**, 135 (2007).
- [2] I. L. Chuang and Y. Yamamoto, Simple quantum computer, *Phys. Rev. A* **52**, 3489 (1995).
- [3] E. Knill, R. Laflamme, and G. J. Milburn, A scheme for efficient quantum computation with linear optics, *Nature* **409**, 46 (2001).
- [4] G. J. Milburn, Quantum optical fredkin gate, *Phys. Rev. Lett.* **62**, 2124 (1989).
- [5] J. H. Shapiro, Single-photon kerr nonlinearities do not help quantum computation, *Phys. Rev. A* **73**, 062305 (2006).
- [6] M. Pant, D. Towsley, D. Englund, and S. Guha, Percolation thresholds for photonic quantum computing, *Nat. Commun.* **10**, 1070 (2019).
- [7] F. Ewert and P. van Loock, 3/4-efficient bell measurement with passive linear optics and unentangled ancillas, *Phys. Rev. Lett.* **113**, 140403 (2014).
- [8] S. Bartolucci, P. Birchall, H. Bombín, H. Cable, C. Dawson, M. Gimeno-Segovia, E. Johnston, K. Kieling, N. Nickerson, M. Pant, F. Pastawski, T. Rudolph, and C. Sparrow, Fusion-based quantum computation, *Nature Communications* **14**, 912 (2023).
- [9] W. Qin, A. F. Kockum, C. S. Muñoz, A. Miranowicz, and F. Nori, Quantum amplification and simulation of strong and ultrastrong coupling of light and matter, *Physics Reports* **1078**, 1 (2024), quantum amplification and simulation of strong and ultrastrong coupling of light and matter.
- [10] M. Bartkowiak, L.-A. Wu, and A. Miranowicz, Quantum circuits for amplification of kerr nonlinearity via quadrature squeezing, *Journal of Physics B: Atomic, Molecular and Optical Physics* **47**, 145501 (2014).
- [11] C. Arenz, D. I. Bondar, D. Burgarth, C. Cormick, and H. Rabitz, Amplification of quadratic hamiltonians, *Quantum* **4**, 271 (2020).
- [12] S. C. Burd, H. M. Knaack, R. Srinivas, C. Arenz, A. L. Collopy, L. J. Stephenson, A. C. Wilson, D. J. Wineland, D. Leibfried, J. J. Bollinger, D. T. C. Allcock, and D. H. Slichter, Experimental speedup of quantum dynamics through squeezing, *PRX Quantum* **5**, 020314 (2024).
- [13] See supplemental material at.
- [14] N. Budinger, A. Furusawa, and P. van Loock, All-optical quantum computing using cubic phase gates, *Phys. Rev. Res.* **6**, 023332 (2024).
- [15] F. Hanamura, W. Asavanant, H. Nagayoshi, A. Sakaguchi, R. Ide, K. Fukui, P. van Loock, and A. Furusawa, Implementing arbitrary multimode continuous-variable quantum gates with fixed non-gaussian states and adaptive linear optics, *Phys. Rev. A* **110**, 022614 (2024).
- [16] M. A. Nielsen and I. L. Chuang, *Quantum Computation and Quantum Information: 10th Anniversary Edition* (Cambridge University Press, 2010).
- [17] T. C. Ralph and G. J. Pryde, Optical quantum computation, *Progress in Optics* **54**, 209 (2011).
- [18] D. Burgarth, N. Galke, A. Hahn, and L. van Luijk, State-dependent trotter limits and their approximations, *Phys. Rev. A* **107**, L040201 (2023).
- [19] L. van Luijk, N. Galke, A. Hahn, and D. Burgarth, Error bounds for lie group representations in quantum mechanics, *Journal of Physics A: Mathematical and Theoretical* **57**, 105301 (2024).
- [20] D. Burgarth, P. Facchi, A. Hahn, M. Johnsson, and K. Yuasa, Strong error bounds for trotter and strangsplittings and their implications for quantum chemistry, *Phys. Rev. Res.* **6**, 043155 (2024).
- [21] H.-P. Breuer and F. Petruccione, *The theory of open quantum systems* (Oxford University Press, USA, 2002).
- [22] M. Takeoka and S. Guha, Capacity of optical communication in loss and noise with general quantum gaussian receivers, *Phys. Rev. A* **89**, 042309 (2014).
- [23] V. Venkataraman, K. Saha, and A. L. Gaeta, Phase modulation at the few-photon level for weak-nonlinearity-based quantum computing, *Nature Photonics* **7**, 138 (2013).
- [24] F. Amrani, J. H. Osório, F. Delahaye, F. Giovanardi, L. Vincetti, B. Debord, F. Gérôme, and F. Benabid, Low-loss single-mode hybrid-lattice hollow-core photonic-crystal fibre, *Light: Science & Applications* **10**, 7 (2021).
- [25] M. Am-Shallem, A. Levy, I. Schaefer, and R. Kosloff, Three approaches for representing lindblad dynamics by a matrix-vector notation, arXiv preprint arXiv:1510.08634 (2015).
- [26] H. Liu, M. L. Iu, N. Hamdash, and A. S. Helmy, Entanglement assisted squeezed states of light in all fiber form-factor, arXiv preprint arXiv:2406.19991 (2024).
- [27] T. Kashiwazaki, T. Yamashima, K. Enbutsu, T. Kazama, A. Inoue, K. Fukui, M. Endo, T. Umeki, and A. Furu-

- sawa, Over-8-dB squeezed light generation by a broadband waveguide optical parametric amplifier toward fault-tolerant ultra-fast quantum computers, *Applied Physics Letters* **122** (2023).
- [28] M. Rosenbluh and R. M. Shelby, Squeezed optical solitons, *Phys. Rev. Lett.* **66**, 153 (1991).
- [29] B. Debord, A. Amsanpally, M. Chafer, A. Baz, M. Maurel, J. M. Blondy, E. Hugonnot, F. Scol, L. Vincetti, F. Gérôme, and F. Benabid, Ultralow transmission loss in inhibited-coupling guiding hollow fibers, *Optica* **4**, 209 (2017).
- [30] K. Bergman and H. A. Haus, Squeezing in fibers with optical pulses, *Opt. Lett.* **16**, 663 (1991).
- [31] M. J. Potasek and B. Yurke, Squeezed light generation in a monomode optical fiber, in *Annual Meeting Optical Society of America* (Optica Publishing Group, 1987) p. ME10.
- [32] C. Perrella, P. S. Light, J. D. Anstie, F. Benabid, T. M. Stace, A. G. White, and A. N. Luiten, High-efficiency cross-phase modulation in a gas-filled waveguide, *Phys. Rev. A* **88**, 013819 (2013).
- [33] N. Matsuda, R. Shimizu, Y. Mitsumori, H. Kosaka, and K. Edamatsu, Observation of optical-fibre Kerr nonlinearity at the single-photon level, *Nature photonics* **3**, 95 (2009).
- [34] K. Inoue, H. Oda, N. Ikeda, and K. Asakawa, Enhanced third-order nonlinear effects in slowlight photonic-crystal slab waveguides of linedefect, *Opt. Express* **17**, 7206 (2009).
- [35] T. Kashiwazaki, N. Takanashi, T. Yamashima, T. Kazama, K. Enbutsu, R. Kasahara, T. Umeki, and A. Furusawa, Continuous-wave 6-dB-squeezed light with 2.5-thz-bandwidth from single-mode p1n waveguide, *APL Photonics* **5** (2020).
- [36] M. Pysher, R. Bloomer, C. M. Kaleva, T. D. Roberts, P. Battle, and O. Pfister, Broadband amplitude squeezing in a periodically poled ktiopo4 waveguide, *Opt. Lett.* **34**, 256 (2009).
- [37] P.-K. Chen, I. Briggs, S. Hou, and L. Fan, Ultra-broadband quadrature squeezing with thin-film lithium niobate nanophotonics, *Opt. Lett.* **47**, 1506 (2022).
- [38] Y. Zhang, C. Husko, S. Lefrancois, I. H. Rey, T. F. Krauss, J. Schröder, and B. J. Eggleton, Cross-phase modulation-induced spectral broadening in silicon waveguides, *Opt. Express* **24**, 443 (2016).
- [39] I.-W. Hsieh, X. Chen, J. I. Dadap, N. C. Panoiu, R. M. Osgood, S. J. McNab, and Y. A. Vlasov, Cross-phase modulation-induced spectral and temporal effects on co-propagating femtosecond pulses in silicon photonic wires, *Opt. Express* **15**, 1135 (2007).
- [40] C. Cui, L. Zhang, and L. Fan, In situ control of effective Kerr nonlinearity with Pockels integrated photonics, *Nature Physics* **18**, 497 (2022).
- [41] L. Chang, M. H. P. Pfeiffer, N. Volet, M. Zervas, J. D. Peters, C. L. Manganelli, E. J. Stanton, Y. Li, T. J. Kippenberg, and J. E. Bowers, Heterogeneous integration of lithium niobate and silicon nitride waveguides for wafer-scale photonic integrated circuits on silicon, *Opt. Lett.* **42**, 803 (2017).
- [42] K. Liu, N. Jin, H. Cheng, N. Chauhan, M. W. Puckett, K. D. Nelson, R. O. Behunin, P. T. Rakich, and D. J. Blumenthal, Ultralow 0.034 dB/m loss wafer-scale integrated photonics realizing 720 million q and 380  $\mu$ W threshold Brillouin lasing, *Opt. Lett.* **47**, 1855 (2022).
- [43] The overall loss rate is computed through the minimum attenuation rate =  $1.6 \times 10^{-5}$  dB/cm reported in [24] for a hollow-core photonic crystal fiber, assuming a fiber with a total length of 36 cm. We further note that the attenuation rate reported in [24] has been demonstrated for a field at 1050 nm wavelength, whereas the cross-Kerr modulated phase shift in [23] is observed in a field at  $\approx$  780 nm.
- [44] N. Matsuda, R. Shimizu, Y. Mitsumori, H. Kosaka, A. Sato, H. Yokoyama, K. Yamada, T. Watanabe, T. Tsuchizawa, H. Fukuda, S. Itabashi, and K. Edamatsu, All-optical phase modulations in a silicon wire waveguide at ultralow light levels, *Applied Physics Letters* **95**, 171110 (2009).
- [45] Z. Li, R. N. Wang, G. Lihachev, J. Zhang, Z. Tan, M. Churayev, N. Kuznetsov, A. Siddharth, M. J. Beryhi, J. Riemensberger, *et al.*, High density lithium niobate photonic integrated circuits, *Nature Communications* **14**, 4856 (2023).
- [46] M. Churayev, R. N. Wang, A. Riedhauser, V. Snigirev, T. Blésin, C. Möhl, M. H. Anderson, A. Siddharth, Y. Popoff, U. Drechsler, *et al.*, A heterogeneously integrated lithium niobate-on-silicon nitride photonic platform, *Nature communications* **14**, 3499 (2023).
- [47] D. Gottesman, A. Kitaev, and J. Preskill, Encoding a qubit in an oscillator, *Phys. Rev. A* **64**, 012310 (2001).
- [48] D. Su, C. R. Myers, and K. K. Sabapathy, Conversion of Gaussian states to non-Gaussian states using photon-number-resolving detectors, *Phys. Rev. A* **100**, 052301 (2019).
- [49] S. Guha, Structured optical receivers to attain superadditive capacity and the Holevo limit, *Phys. Rev. Lett.* **106**, 240502 (2011).
- [50] M. M. Wilde and S. Guha, Polar codes for classical-quantum channels, *IEEE Transactions on Information Theory* **59**, 1175 (2013).
- [51] M. R. Grace, C. N. Gagatsos, and S. Guha, Entanglement-enhanced estimation of a parameter embedded in multiple phases, *Phys. Rev. Res.* **3**, 033114 (2021).
- [52] J. Bringewatt, I. Boettcher, P. Niroula, P. Bienias, and A. V. Gorshkov, Protocols for estimating multiple functions with quantum sensor networks: Geometry and performance, *Phys. Rev. Res.* **3**, 033011 (2021).
- [53] M. Reed, B. Simon, and S. Reed, *Methods of Modern Mathematical Physics: Fourier Analysis, Self-Adjointness* (世界图书出版公司, 2003).

## Supplemental Material

In this supplemental material, we give the explicit form of the squeezing sequence when squeezing is applied to both modes, derive the bound given in Eq. (6) in the main body of the manuscript and investigate its tightness, and give more details for the photon loss model considered in the manuscript.

### A: Single-mode squeezing applied to two modes

By applying single-mode squeezing transformations  $S_{x,\theta}$  to both modes, where  $x \in \{a, b\}$  indicates which mode is squeezed, the cross-Kerr interaction can be amplified by a factor of  $\cosh^2(2r)$ . The corresponding squeezing sequence reads

$$\lim_{N \rightarrow \infty} \left( S_{a,0}^\dagger S_{b,0}^\dagger U_{\Delta t} S_{a,0} S_{b,0} S_{a,\pi}^\dagger S_{b,\pi}^\dagger U_{\Delta t} S_{a,\pi} S_{b,\pi} S_{a,0}^\dagger S_{b,\pi}^\dagger U_{\Delta t} S_{a,0} S_{b,\pi} S_{a,\pi}^\dagger S_{b,\pi}^\dagger U_{\Delta t} S_{a,\pi} S_{b,\pi} \right)^N = e^{-i \cosh^2(2r) H t}, \quad (\text{A1})$$

where  $\Delta t = \frac{t}{4N}$ .

### B: Bounding the Trotter error

Here we derive the upper bound for the gate error  $\epsilon_N(\phi)$  given in (6) in the main body of the manuscript using the state-dependent Trotter bounds for unbounded Hamiltonians from [20]. In particular, we will make use of the Theorem:

**Theorem 1:** *Let  $H_1$  be self-adjoint on  $D(H_1)$  and  $H_2$  be self-adjoint on  $D(H_2)$ . Let  $|\varphi\rangle$  be an eigenstate of  $H = H_1 + H_2$  with eigenvalue  $h$ , i.e.,  $H|\varphi\rangle = h|\varphi\rangle$ . If  $|\varphi\rangle \in D(H_1^2) \cap D(H_2^2)$ , then*

$$\epsilon_N(t; |\varphi\rangle) \leq \frac{t^2}{2N} \left( \|(H_1 - g)^2 |\varphi\rangle\| + \|(H_2 - h + g)^2 |\varphi\rangle\| \right), \quad (\text{B1})$$

for all  $t, g \in \mathbb{R}$ , and the Trotter product formulae converges on  $|\varphi\rangle$ .

Here, the Trotter error  $\epsilon_N(t; |\varphi\rangle)$  is given by

$$\epsilon_N(t; |\varphi\rangle) = \left\| \left( e^{-iHt} - \left( e^{-iH_1 \frac{t}{N}} e^{-iH_2 \frac{t}{N}} \right)^N \right) |\varphi\rangle \right\|, \quad (\text{B2})$$

where  $\|\cdot\|$  denotes the Euclidean vector norm.

Before we apply Theorem 1, we first show that the domain assumptions are satisfied. We identify

$$\begin{aligned} H_1 &= S_0^\dagger H S_0 = \chi \left( \cosh(2r) a^\dagger a - \frac{\sinh(2r)}{2} (a^\dagger a^\dagger + aa) \right) b^\dagger b, \\ H_2 &= S_\pi^\dagger H S_\pi = \chi \left( \cosh(2r) a^\dagger a + \frac{\sinh(2r)}{2} (a^\dagger a^\dagger + aa) \right) b^\dagger b. \end{aligned} \quad (\text{B3})$$

and define the space of finite excitations by

$$\mathcal{F} = \left\{ |\varphi\rangle \in L^2(\mathbb{R}^2) \mid \exists N, M \in \mathbb{N} : |\varphi\rangle = \sum_{k=0}^N \sum_{\ell=0}^M c_{k\ell} |k\ell\rangle \right\},$$

where  $|k\ell\rangle$  are the fock states of mode  $a$  and mode  $b$ . We first show that  $\mathcal{F}$  is a set of analytic vectors of the Hamiltonians,

$$H = (\alpha a^\dagger a + \beta (a^\dagger a^\dagger + aa)) b^\dagger b \quad (\text{B4})$$

with  $\alpha, \beta \in \mathbb{R}$ , noting that  $H_1$  and  $H_2$  defined above are of this form.

We use the definition of analytic vectors  $|\varphi\rangle$  in [53] (Section X.6, p201),

$$\sum_{n=0}^{\infty} \frac{\|H^n |\varphi\rangle\|}{n!} t^n < \infty$$

for some  $t > 0$ . Let  $\gamma = \max\{|\alpha|, |\beta|\}$  and for a fixed  $|\varphi\rangle \in \mathcal{F}$  and let  $K = \max\{N, M\}$ . Then

$$H^n |k\ell\rangle = (\alpha a^\dagger a + \beta(a^\dagger a^\dagger + aa))^{2n} \ell^n |k\ell\rangle$$

and

$$\|H^n |\varphi\rangle\| \leq \gamma^n 3^n \sqrt{\frac{(K+2n)!}{K!}} K^n$$

where we upper bounded the expansion of operators by the worst case where only strings of creation operators with  $(a^\dagger)^{2n} |K\rangle = \sqrt{\frac{(K+2n)!}{K!}} |K+2n\rangle$  on the first mode appear, and upper bounded the contributions from  $|\varphi\rangle$  by its highest number  $K$  of photons. Now let

$$c_n = \frac{(3\gamma K t)^n \sqrt{\frac{(K+2n)!}{K!}}}{n!},$$

then

$$\frac{c_{n+1}}{c_n} = \frac{(3\gamma K t) \sqrt{(K+2n+2)(K+2n+1)}}{(n+1)} \rightarrow 6\gamma K t$$

and by the ratio test the series converges for  $t < \frac{1}{6\gamma K}$ . Consequently, any  $|\varphi\rangle \in \mathcal{F}$  is an analytic vector of  $H$  given in Eq. (B4).

We note that  $H$  being essentially self-adjoint on  $\mathcal{F}$  follows from Corollary 2 in [53] (Section X.6, p202), where  $H\mathcal{F} = \mathcal{F}$  follows from the fact that  $H$  maximally creates two new photons and the denseness of  $\mathcal{F}$  is used. In abuse of notation, we denote the closure of  $H$  on  $\mathcal{F}$  also as  $H$ .

By definition, for some self-adjoint  $H$  the operator  $H^2$  is the self-adjoint operator with domain  $D(H^2) = \{|\psi\rangle \in D(H) \mid H|\psi\rangle \in D(H)\}$ . Since  $\mathcal{F} \in D(H)$  and  $H\mathcal{F} \in D(H)$ , any  $|\varphi\rangle \in \mathcal{F}$  is in  $D(H^2)$ .

In order to apply Theorem 1 to upper bound the gate error  $\epsilon_N(\phi)$ , we first notice that

$$\begin{aligned} \epsilon_N(\phi) &= \left\| P \left( CZ(\phi) - (e^{-iH_1 \Delta t} e^{-iH_2 \Delta t})^N \right) P \right\|_{\text{HS}} \\ &\leq \sqrt{\sum_{x \in \{0,1\}^2} \left\| \left( CZ(\phi) - (e^{-iH_1 \frac{t}{2N}} e^{-iH_2 \frac{t}{2N}})^N \right) |x\rangle \right\|^2} \end{aligned} \quad (\text{B5})$$

where we used that for any operator  $A$  we have,

$$\begin{aligned} \|PAP\|_{\text{HS}} &= \sqrt{\text{Tr}(PA^\dagger PAP)} \\ &= \sqrt{\sum_{x \in \{0,1\}^2} \langle x | A^\dagger P A | x \rangle} \\ &\leq \sqrt{\sum_{x \in \{0,1\}^2} \|A|x\rangle\|^2}. \end{aligned} \quad (\text{B6})$$

We now can use Theorem 1 to further upper bound the right-hand side to obtain

$$\epsilon_N(\phi) \leq \sqrt{\sum_{x \in \{0,1\}^2} (\|H_1^2 |x\rangle\| + \|(H_2 - h_x)^2 |x\rangle\|)^2}, \quad (\text{B7})$$

where we picked  $g = 0$  in (B1) and  $h_x$  is the eigenvalue of  $H$  that corresponds to the eigenstate  $|x\rangle$ . We note that  $h_x = 0$  for  $x \in \{00, 01, 10\}$  and  $h_{11} = 2\chi \cosh(2r)$ . Since  $\|H_1^2 |00\rangle\| = \|H_1^2 |10\rangle\| = \|H_2^2 |00\rangle\| = \|H_2^2 |10\rangle\| = 0$  we further find that

$$\epsilon_N(\phi) \leq \sqrt{(\|H_1^2 |01\rangle\| + \|H_2^2 |01\rangle\|)^2 + (\|H_1^2 |11\rangle\| + \|(H_2 - h_{11})^2 |11\rangle\|)^2}. \quad (\text{B8})$$

As

$$\|H_1^2 |01\rangle\| = \left\| \frac{\chi^2 \sinh^2(2r)}{2} |01\rangle - \sqrt{2}\chi^2 \sinh(2r) \cosh(2r) |21\rangle + \frac{\sqrt{6}\chi^2 \sinh^2(2r)}{2} |41\rangle \right\|, \quad (\text{B9})$$

$$\|H_2^2 |01\rangle\| = \left\| \frac{\chi^2 \sinh^2(2r)}{2} |01\rangle + \sqrt{2}\chi^2 \sinh(2r) \cosh(2r) |21\rangle + \frac{\sqrt{6}\chi^2 \sinh^2(2r)}{2} |41\rangle \right\|, \quad (\text{B10})$$

and

$$\|H_1^2 |11\rangle\| = \left\| \left( \chi^2 \cosh^2(2r) + \frac{3\chi^2 \sinh^2(2r)}{2} \right) |11\rangle - 2\sqrt{6}\chi^2 \sinh(2r) \cosh(2r) |31\rangle + \frac{\sqrt{30}\chi^2 \sinh^2(2r)}{2} |51\rangle \right\|, \quad (\text{B11})$$

$$\begin{aligned} \|(H_2 - h_{11})^2 |11\rangle\| = & \left\| \left( \chi^2 \cosh^2(2r) - 2h_{11}\chi \cosh(2r) + \frac{3\chi^2 \sinh^2(2r)}{2} + h_{11}^2 \right) |11\rangle \right. \\ & \left. + \left( 2\sqrt{6}\chi^2 \sinh(2r) \cosh(2r) - \sqrt{6}h_{11}\chi \sinh(2r) \right) |31\rangle + \frac{\sqrt{30}\chi^2 \sinh^2(2r)}{2} |51\rangle \right\|, \end{aligned} \quad (\text{B12})$$

we arrive at the final result

$$\epsilon_N(\phi) \leq \frac{\chi^2 t^2 \cosh^2(2r)}{8N} f(r), \quad (\text{B13})$$

where

$$\begin{aligned} f(r) = & \left[ 7 \tanh^4(2r) + 8 \tanh^2(2r) + \frac{1}{4} \left( (4 + 108 \tanh^2(2r) + 39 \tanh^4(2r))^{\frac{1}{2}} + (4 + 12 \tanh^2(2r) \right. \right. \\ & \left. \left. + 39 \tanh^4(2r))^{\frac{1}{2}} \right)^2 \right]^{\frac{1}{2}}. \end{aligned} \quad (\text{B14})$$

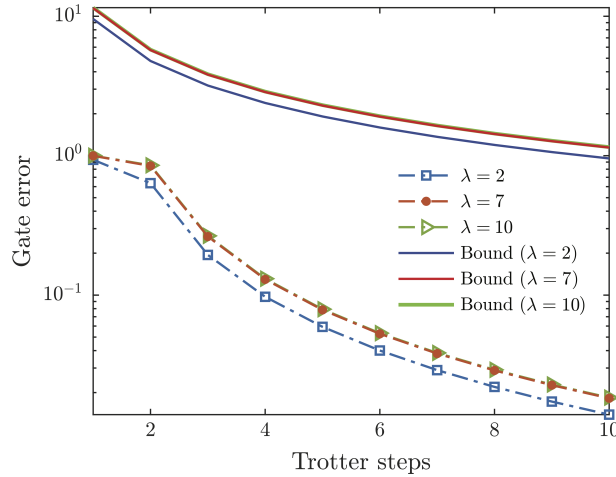


Figure 3. Gate error (6) shown as dashed lines for implementing controlled phase gate  $\text{CZ}(\pi)$  as a function of the number of Trotter steps  $N$  for different values of the cross-Kerr phase shift  $\chi t = \frac{\pi}{2}, \frac{\pi}{7}, \frac{\pi}{10}$  for different amplification factors  $\lambda = 2, 7, 10$ . The corresponding upper bounds given by (B14) are shown as solid lines. The gate errors were normalized to 1 by dividing by its largest value. For comparison, the upper bounds were also normalized by dividing by the corresponding largest gate error.

Next, we analyze the tightness of the upper bound (B13). In Fig. 3 we plot the gate errors (dot-dashed lines) to implement the controlled phase gate  $\text{CZ}(\pi)$  for different cross-Kerr phase shifts  $\chi t = \frac{\pi}{2}, \frac{\pi}{7}, \frac{\pi}{10}$  that are amplified by the factor  $\lambda = 2$  (blue squares), 7 (red circles) and 10 (green triangles), respectively. The corresponding upper bounds are shown as solid lines.

### C: Photon loss model

We model photon losses by coupling each mode via a beam splitter interaction to auxiliary modes  $c$  and  $d$ . The total Hamiltonian including the cross-Kerr interaction is given by

$$H = \chi a^\dagger ab^\dagger b + g(ac^\dagger + a^\dagger c) + g(bd^\dagger + b^\dagger d), \quad (\text{C1})$$

where  $c, d$  ( $c^\dagger, d^\dagger$ ) are the annihilation and creation operators of the auxiliary modes and  $g$  is the coupling strength. If we assume that the auxiliary modes are in the vacuum state  $|00\rangle$ , after each time step  $\Delta t = \frac{1}{4N}$  of the amplification sequence given in Eq. (A1) the dynamics of the two modes  $a$  and  $b$  is given by the quantum channel,

$$\mathcal{E}_{\Delta t}^{(j)}(\cdot) = \text{Tr}_{cd} [e^{-iH_j \Delta t} ((\cdot) \otimes |00\rangle \langle 00|) e^{iH_j \Delta t}], \quad (\text{C2})$$

where  $\text{Tr}_{cd}$  denotes the partial trace over the auxiliary modes and  $H_j = S_j^\dagger H S_j$ ,  $S_j \in \{S_{a,\alpha} S_{b,\beta} : j \in \{1, 2, 3, 4\}, \alpha = \pi \lfloor \frac{j-1}{2} \rfloor, \beta = \pi(j-1) \bmod 2\}$ . If we introduce the loss rate  $\eta t$  via choosing  $g^2 \Delta t^2 = \eta \Delta t$ , we obtain for  $j = 1, 2$  the quantum channels

$$\mathcal{E}_{\Delta t}^{(j)} = \text{id} + \Delta t \mathcal{H}_j + \Delta t \left( \cosh^2(r) \mathcal{L}_l + \sinh^2(r) \mathcal{L}_h - \frac{\sinh(2r)}{2} (\mathcal{K}_a \pm \mathcal{K}_b) \right) + \mathcal{O}\left(\frac{1}{N^2}\right), \quad (\text{C3})$$

where  $\mathcal{H}_j = -i[H_j, \cdot]$ ,  $\mathcal{L}_l = \eta(\mathcal{D}_a + \mathcal{D}_b)$  and  $\mathcal{L}_h = \eta(\mathcal{D}_{a^\dagger} + \mathcal{D}_{b^\dagger})$  are formed by Lindblad operators of the form  $\mathcal{D}_L$ , given in the main body of the manuscript, and we defined the super operators

$$\mathcal{K}_L(\cdot) = \eta \left( L(\cdot)L + \frac{1}{2} (L^2(\cdot) + (\cdot)L^2) + L^\dagger(\cdot)L^\dagger + \frac{1}{2} (L^{\dagger 2}(\cdot) + (\cdot)L^{\dagger 2}) \right). \quad (\text{C4})$$

Similarly, for  $j = 3, 4$  we obtain

$$\mathcal{E}_{\Delta t}^{(j)} = \text{id} + \Delta t \mathcal{H}_j + \Delta t \left( \cosh^2(r) \mathcal{L}_l + \sinh^2(r) \mathcal{L}_h + \frac{\sinh(2r)}{2} (\mathcal{K}_a \mp \mathcal{K}_b) \right) + \mathcal{O}\left(\frac{1}{N^2}\right). \quad (\text{C5})$$

As such, the sequence of quantum channels  $\left(\prod_{j=1}^4 \mathcal{E}_{\Delta t}^{(j)}\right)^N$  is in the limit of infinitely many Trotter steps  $N$  given by

$$\begin{aligned} \lim_{N \rightarrow \infty} \left( \prod_{j=1}^4 \mathcal{E}_{\Delta t}^{(j)} \right)^N &= \exp\left(\frac{t}{4} \sum_{j=1}^4 (\mathcal{H}_j) + t \cosh^2(r) \mathcal{L}_l + t \sinh^2(r) \mathcal{L}_h\right) \\ &= \exp\left([\cosh^2(2r) \mathcal{H} + \cosh^2(r) \mathcal{L}_l + \sinh^2(r) \mathcal{L}_h] t\right). \end{aligned} \quad (\text{C6})$$

In Fig. 4 we investigate the dynamics for finite  $N$  by analyzing the error

$$\epsilon = \left\| \mathcal{E}_t - \left( \prod_{j=1}^4 \mathcal{E}_{\Delta t}^{(j)} \right)^N \right\|_{\text{HS}} \quad (\text{C7})$$

between the quantum channel  $\mathcal{E}_t$ , obtained for  $N \rightarrow \infty$ , and the sequence of quantum channels  $\left(\prod_{j=1}^4 \mathcal{E}_{\Delta t}^{(j)}\right)^N$  where the quantum channels  $\mathcal{E}_{\Delta t}^{(j)}$  are given in (C2). We study the error (C7) between the two evolutions for different phase shifts  $\phi = \frac{\pi}{100}, \frac{\pi}{50}, \frac{\pi}{10}$  obtained by amplifying the bare phase shift  $\chi t = 1.2 \times 10^{-3}$  for a loss rate  $\eta t = 5.76 \times 10^{-4}$  dB [23, 24] for different number of Trotters steps  $N$ .

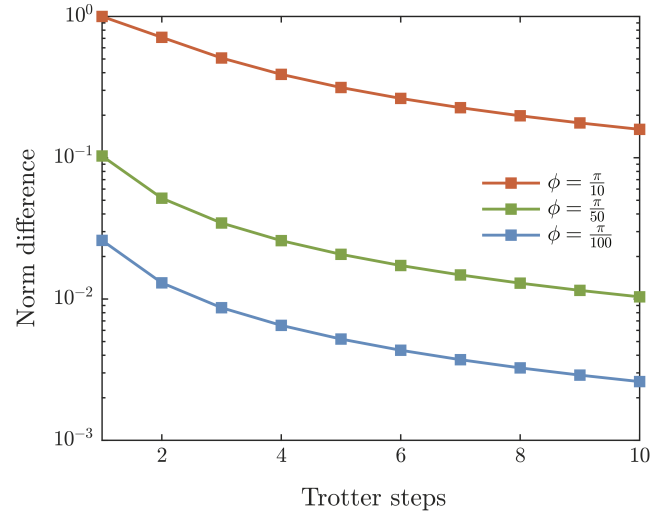


Figure 4. Norm difference (C7) for different phase shifts as a function of the number of Trotter steps  $N$ . We used  $\chi t = 1.2 \times 10^{-3}$  for the bare phase shift and  $\eta t = 5.76 \times 10^{-4}$  dB for the loss rate [23, 24]. For each curve, the norm difference was normalized to 1 by dividing by its largest value.